ECC
Eurasian Chemical Communications
Original Research Article
http://echemcom.com

Preparing hierarchical nanoporous ZSM-5 zeolite *via* post-synthetic modification of zeolite synthesized from bagasse and its application for removal of Pb2+

Sedigheh Rostami[a], Seyed Naser Azizi [a,b,*], Neda Asemi[a]

[a]*Analytical division, Faculty of Chemistry, University of Mazandaran, Postal code 47416-95447, Babolsar, Iran*

[b]*Nano and Biotechnology Research Group, University of Mazandaran, Mazandaran, Babolsar, Iran*

Received: 26 February 2017, Accepted: 6 November 2017, Published: 1 January 2019

Abstract

In this study, hierarchical H-ZSM-5 zeolite is prepared *via* post-synthetic modification of parent H-ZSM-5 zeolite (Si/Al=35) synthesized from bagasse (BGA) as silica source using desilication with alkaline treatment (AT). For optimizing the effective parameters on desilication, Taguchi method was utilized. Cultivated BGA in the south of the Caspian Sea (Mazandaran province, Iran) is applied for extracting silica powder and used in the synthesis of zeolite. In this work, two responses have been considered. The First and the second responses are the maximum amounts of extracted silicone and the removal of Pb^{2+} % from aqueous solutions, respectively. For this purpose, the effect of four important factors with three selected levels including; concentration of NaOH solution (0.1, 0.2 and 0.5 M), temperature (25, 55 and 85 C°), time of reflux (30, 60 and 120 min) and molar ratio of TMAOH/ NaOH (0.5, 1 and 1.5) are studied on both of the responses. TMAOH was defined as tetra methyl ammonium hydroxide. According to Taguchi method, the optimum conditions for both responses are concluding as Concentration of NaOH solution=0.2 M, temperature =55 C°, time of reflux=120 min and molar ratio of TMAOH/ NaOH=0.5. The results display that Concentration of NaOH solution in comparison to other factors is the most effective one in both responses. Also, AT-05-ZSM-5 is selected as the optimum zeolite with volumes 278.13 ppm and 90.2 % with S/N ratios 48.878 and 39.097 for the first and the second responses, respectively. Parent H-ZSM-5 and AT-05-ZSM-5 are characterized by x-ray diffraction (XRD), scanning electronic microscopy (SEM), Fourier transform infra-red (IR), Brunauer–Emmett–Teller (BET), Barrett-Joyner-Halenda (BJH) and inductively coupled plasma-optical emission spectrometery (ICP-OES). AT-05- ZSM-5 demonstrates a limit and uniform meso-pore average size distribution at 7.65 nm using alkaline treatment.

Keywords: Bagasse; ZSM-5 zeolite; hierarchical ZSM-5 zeolite; desilication; Taguchi method; removal of Pb^{2+}.

Introduction

ZSM-5 zeolites are microporous molecular sieves that have excellent properties related to intrinsic acidity and uniform micro-pores with many applications in catalysis and separation processes [1-3]. However, the microporous network of zeolites

*Corresponding author: Seyed Naser Azizi
Tel: +98 (11) 35302350, Fax: +98 (11) 35302350
E-mail: azizi@umz.ac.ir

frequently results in intra crystalline diffusion limitations as a result of the difficult gas transport of reactants to the active sites in the channels or back-diffusion of products [4-6]. Development of more open structures by creating additional porosity, *e.g.* combining micro- and meso-pores, has a high potential to significantly improve the diffusional properties. Porous materials like hierarchical zeolites are generally obtained by new developed synthesis procedures such as post-synthesis treatments of microporous parent materials. Examples of new synthesis procedures are in the literatures [7,8]. Post-synthesis treatments of parent zeolites create certain extra porosity due to the formation of defect sites in the zeolite framework [8]. The diffusion limitation in zeolites (micro-pores) can be minimized by enlarging pore size post-synthesis modification techniques [9-11]: reducing zeolite crystal size, enlarging zeolites pores, carbon-templated synthesis, desilication and dealumination [12]. Alkaline treatment, which is referenced as desilication in the literatures, [13-15] has been introduced as an effective approach for creating extra pores and modifying the acidity in high-silicon zeolites, such as parent H-ZSM-5 [16]. In this work, Bagasse (BGA) was utilized as a low-cost silica source because of having high silica value to synthesize parent H-ZSM-5 zeolite. As an important number of the porous family materials, zeolite has been adopted in many industrial and biological applications, such as removal of toxic metal ions [17]. Among heavy metals, Pb^{2+} ion is one of the most poisonous heavy metal ions that accumulate in muscles, bones, kidney and brain tissues. It has the potential to cause various disorders and has been regarded as the priority controlled pollutant in many countries [18]. The resultant higher concentrations of the lead in the ecosystem have substantial impacts on the environment and human health [19]. For this reason, removal of the lead ions in the aqueous solution using prepared hierarchical H-ZSM-5 was studied. Many different treatment techniques such as chemical precipitation, coagulation–precipitation, adsorption and ion exchange have been developed to remove heavy metals from contaminated water [20-22].These methods usually involve expensive materials and high operation costs. Among all of these approaches, the adsorption process is considered more efficient and economical because of its flexibility in design, simplicity of operation, facile handling, and in many cases generation of high-quality treated effluent [23]. Much work has been done on the removal of the lead by clays, minerals such as calcite, calcareous soils, some industrial by-products and waste materials such as sludge, chitosan, dead biomass, modified wool, moss, peat, seaweed, and zeolite [25, 26]. Among the different minerals, which possess sorbent properties, zeolites appear to be one of the most promising sorbents for this purpose [25]. The ZSM-5 zeolite has the given chemical composition: $Na_2O{:}Al_2O_3{:}\ 2nSiO_2{:}\ xH_2O$ with n higher or equal six and consists of interconnected cylindrical channels containing openings between 5.1 and 5.6 Å of two different types [26]. Taguchi's optimization technique is a unique and powerful optimization discipline that allows optimization with minimum number of experiments. The Taguchi experimental design reduces cost, improves quality, and provides robust design solutions [27,28]. This method is capable of establishing an optimal

design configuration even when significant interaction exists between and among the control variables [29]. Totally, the main objective in this study is statistically post-synthetic modification parent H-ZSM-5 zeolite by desilication in order to prepare hierarchical H-ZSM-5 zeolite using Taguchi experimental design and selecting optimum conditions for both of the responses. Parent H-ZSM-5 and AT-05-ZSM-5 are characterized by x-ray diffraction (XRD), scanning electronic microscopy (SEM), Fourier transform infra-red (IR), Brunauer–Emmett–Teller (BET), Barrett-Joyner-Halenda (BJH) and inductively coupled plasma-optical emission spectrometery (ICP-OES).

Experimental section

Material

Sodium aluminate ($NaAlO_2$) was purchased from Sigma-Aldrich and used as alumina source. White SiO_2 powder was extracted from BGA (prepared from the south of the Caspian Sea (Bahnamir, Mazandaran province, Iran) according to procedure reported by Kalapathy et al. [30]. Lead nitrate ($Pb(NO_3)_2$), (Ammonium Chloride) NH_4Cl, NaOH, Tetra methyl ammonium hydroxide (TMAOH) as templating agent and organic base for alkaline treatment were prepared from Merck.

Extraction of silica from BGA

At first, for extraction of silica from BGA, 100 g BGA was manually cleaned and washed with distilled water for removing dust and adhered particles and was subsequently dried in oven in 70 Cº. After that, it was burned in air for obtaining black ash. Then, BGA black ash was calcined in electrical furnace at 550 Cº for 8 h to remove all of organic materials and to obtain white ash. For obtaining pure silica, the calcined withe ash was dissolved in 2 M NaOH for 4 h while boiling at 100 Cº under constant stirring and it was cooled at room temperature. Then, the formed sodium silicate solution was centrifuged and was titrated with HCl 1 M to become neutralized for the formation of silica gel. Silica gel was aged for 24 h in room temperature under constant environmental conditions. Formed silica gel was filtered and washed with distilled water several times in order to give neutralizing gel. Then, the product was dried at 80 Cº for 2 h. For obtaining pure silica powder, a mortar and pestle were used for grinding xero-gel pieces.

Synthesis of parent H-ZSM-5 zeolite

H-ZSM-5 zeolite with Si/Al = 35 was synthesized using TMAOH as a template in an autoclave under autogenous pressure at 180 Cº by conventional hydrothermal method. At first, 0.339 g sodium aluminate ($NaAlO_2$) was dissolved in 2.5 M NaOH solution until complete digestion, then 0.369 mL TMAOH 0.1 M as template was added to it under vigorous stirring for preparing a clear homogenous solution and it was named as solution A. Besides, sodium silicate solution was prepared by dissolving 10 g silica powder in an alkaline solution NaOH 2.5 M under agitation on stirrer and was named solution B. Then, solution B was added dropwise to the solution A. They were mixed together under vigorous agitation for 4 h until a homogeneous gel mixture was obtained. The final gel mixture was then put into the stainless-steel autoclave and crystallization zeolite was carried out for 24 h. The temperature of the autoclave was increased to 180 Cº. The obtained products were washed with deionized water until the pH value of the washing water reached 8, and then dried overnight at 105 Cº. After that the dried sample was converted into ammonium

form by three-time ion exchange with 1 M NH_4Cl at 70 Cº for 5 h. Subsequently, the obtained sample was again filtrated, washed, and dried overnight. Finally, the dried sample was transformed into the hydrogen form through calcination. It is worth mentioning that the solid product was calcined at 500 Cº for 5 h under airflow in order to remove the organic template trapped in the zeolite pores. The initial molar ratio of prepared gel is $70SiO_2$: Al_2O_3: $34Na_2O$: 95 H_2O: 2TMAOH.

General procedure for desilication of parent H-ZSM-5

The synthesized parent H-ZSM-5 was desilicated using AT in all experiments. At first, 0.5 g of H-ZSM-5 was stirred in 15 mL of alkaline solution in a round-bottom flask coupled with a reflux condenser. Then slurry was cooled down immediately using an ice water bath and filtered .At this step, a portion of collected filtrate was kept to be analyzed by ICP-OES. The filtered cake was dried in an air oven at 105 Cº overnight. The resulted zeolite was named AT-ZSM-5.

Taguchi design for desilicating of parent H-ZSM-5

The Taguchi method was utilized to recognize the optimum conditions and to select the factors having the most principal effects on obtaining the maximum amount of extracted silicon of parent H-ZSM-5 and maximum removal of the Pb^{2+} % aqueous solutions. Table 1 shows the four selected factors and the experimental Taguchi method levels used in this study. Each factor was studied at three levels (high, +1, middle, 0 and low, −1). The used level setting values of the main variables (A–D) and the L_9 orthogonal array employed to assign the considered variables are shown in Table 2. Taguchi statistical and experimental designs offer the optimum conditions on the basis of the measured values of the characteristic properties. This capability is one of the advantages of this method over the conventional experimental design methods [31]. Using the orthogonal array particularly designed for the Taguchi method, the optimum experimental conditions can be easily determined [32]. Taguchi optimization method is a powerful tool for the design of a high-quality system. This method provides smaller, less costly experiments that have high rates of reproducibility. It is also useful in studying the interactions between parameters. Compared to the conventional approach of experimentation, this method drastically reduces the number of experimental runs. System design involves the application of scientific and engineering knowledge required in manufacturing a product; parameter design is employed to find optimal settings-process values for improving the performance characteristics and tolerance design consists of determining and analyzing tolerances in the optimal settings recommended by parameter design [33]. This method uses the signal to noise (S/N) ratio to estimate the quality characteristics deviating from the desired values. Usually three types of S/N analysis can be applied: (1) lower is better (LB), (2) nominal is best (NB), and (3) higher is better (HB) [34]. Because the goal of this work is the maximum amount of extracted silicon of parent H-ZSM-5 and the maximize removal of the Pb^{2+} %, the suggested function by the Taguchi for S/N estimation according to the "larger-the-better" was taken as follows [35] by Equation (1)

$$\frac{S}{N} = -10\ log\ \log_{10}[\frac{1}{n}\sum(\frac{1}{PREi})^2] \qquad (1)$$

Where n is the number of repetitions under the same experimental conditions, PRE represents the results of measurements. After the calculation of S/N ratio, the experimental results were analyzed with the help of performance statistics and analysis of variance (ANOVA). After that, optimum condition is predicted using Qualitek-4 software. Finally, to validate the method, a confirmatory experiment was carried out and the differences between predicted and the confirmatory experiment results were evaluated.

Adsorption studies

Nine of H-ZSM-5 zeolite were prepared using Taguchi method and applied as adsorbent of Pb^{2+} from aqueous solutions. In each adsorption experiment run, 15 mL of pb^{2+} solution at pH =6, lead initial concentrations 10 ppm, adsorbent nine ZSM-5 desilicated dosages 0.16 g was shaken at fixed contact time 6 h and in temperature 55 Cº. Afterward, the samples were filtered and analyzed for residual lead ion concentration in solution. The removal of Pb^{2+}% was calculated according to the following equation (2):

$$\boldsymbol{RP\ (Pb^{2+}) = \frac{C_0 - C_t}{C_0} \times 100} \quad (2)$$

Here C_0 and C_t are initial and residual concentrations of Pb^{2+} in the solution (mg L^{-1}) [24].

Instrumentation

X-ray diffraction (XRD) XRD patterns were recorded with an X-ray diffractometer (Shimadzu XD-DL) using Cu-*K*α radiation (λ = 1.5418 Å) at 35kV and 28 mA in the 2θ range from 4º-50º. The chemical composition of silica powder extracted from BGA was analyzed by X-ray fluorescence spectrometry (XRF; 8410 Rh 60kV). The surface morphology and structure measurements were carried out using a field-emission scanning electron microscope (FESEM, KYKY-EM-3200) operating at 15 and 26 kV. All samples were subsequently sputter coated with a thin gold film to reduce the charging effects. Fourier transform Infrared spectrum was collected using a FT-IR spectrophotometer (Bruker Vector 22) in the range of 400–4000 cm^{-1}. Spectra were obtained by the KBr pellet method. N_2 adsorption and desorption isotherms were measured at 77.3 K on a Nova Station A (Quantachrome, 1994-2006, version 2.2, USA) gas sorption analyzer. Total specific surface areas (S_{BET}) were calculated using the Brunauer-Emmett-Teller (BET) method [16], and the total pore volume (V_{total}) was determined from N_2 uptake at a relative N_2 pressure of 0.99. The t-plot method was used to distinguish between micro- and mesoporosity [36]. The t-plot method was employed to evaluate the micro pore surface area (S_{Micro}) and the micro pore volume (V_{Micro}) in the p/p_0 range 0.1-0.4. The mesopore volume (V_{Meso}) was calculated from the discrimination between the V_{Total} and V_{Micro}. The pore size distribution was estimated utilizing the Barrett-Joyner-Halenda (BJH) method [37]. The inductively coupled plasma-optical emission spectroscopy (ICP-OES) (Perkin Elmer Optima 2000 DV ICP-OES) was used to measure the amount of silicon and aluminum filtrates solutions". Pb^{2+} in aqueous solutions was measured by atomic absorption spectrometer (PerkinElmer Analyst 700with wave-length) in wave-length 283.3 nm and current 8 mA with HCL lamp.

Table 1. Experimental design levels of chosen variables for Taguchi method

Factors	Level1	Level2	Level3
A: Concentration of NaOH (M)	0.1	0.2	0.5
B: Temperature (C°)	25	55	85
C: Time of reflux (min)	30	60	120
Molar ratio of TMAOH / NaOH)	0.5	1	1.5

Table 2. The structure of Taguchi's L_9 orthogonal array design and S/N for desilication of parent H-ZSM-5 and results of the measurement for two responses

Number of experiment	sample	A[a]	B[b]	C[c]	D[d]	Removal of Pb^{2+} (%)		S/N for Removal of Pb^{+2}	The value of Extracted Si(mg L^{-1})		S/N for The value of extracted Si
						(r^e=1)	(r^e=2)		(r^e=1)	(r^e=2)	
1	L_1	1	1	1	1	78.81	78.65	37.92	158.00	157.00	43.94
2	L_2	1	2	2	2	79.63	79.35	38.00	176.00	175.00	44.88
3	L_3	1	3	3	3	78.36	78.21	37.87	161.00	160.00	44.10
4	L_4	2	1	2	3	86.06	86.27	37.70	220.00	221.00	46.86
5	L_5	2	2	1	3	90.1	90.2	39.09	278.00	278.00	48.88
6	L_6	2	3	1	2	79.35	79.39	37.99	172.00	173.00	44.73
7	L_7	3	1	3	2	78.91	78.58	37.92	199.00	198.00	45.95
8	L_8	3	2	1	3	79.36	79.2	37.98	201.00	202.00	46.08
9	L_9	3	3	2	1	78.1	78.3	37.86	203.00	202.00	46.12

[a]Concentration of NaOH solution (M)
[b]Temperature (C°)
[c]Time of reflux (min)
[d] Molar ratio of TMAOH / NaOH
r^e =reproducibility of experiments

Results and discussion

Characterization of BGA

The chemical composition of BGA ash in the form of stable oxides was analyzed with X-ray fluorescence (XRF) (Table 3). As it is shown, the major oxide constituent is SiO_2 with purity approximately 86.498% (wt.) along with small amounts of other inorganic oxides was brought in Table3. Because of having a rich source of Si, BGA is selected for the synthesis of parent H- ZSM-5 zeolite with Si/Al=35. Also, Figure 1 shows the XRD pattern of silica extracted from BGA. A broad peak with $2\boldsymbol{\theta} = 24^o$ indicates the formation of amorphous silica without any impurity. Beside, SEM images of BGA ash and SiO_2 extracted from BGA are displayed in

Figure 2 a, b. As it is illustrated, the SEM image of extracted SiO_2 from BGA shows the presence of the spherical particles with average diameter about 35 nm.

Table 3. The chemical composition of BGA ash in the form of stable oxides was analyzed with XRF

Na_2O	MgO	Al_2O_3	SiO_2	P_2O_5	K_2O	CaO	Fe_2O_3
0.220	**1.202**	**3.380**	**86.498**	**6.075**	**2.019**	**0.348**	**0.240**

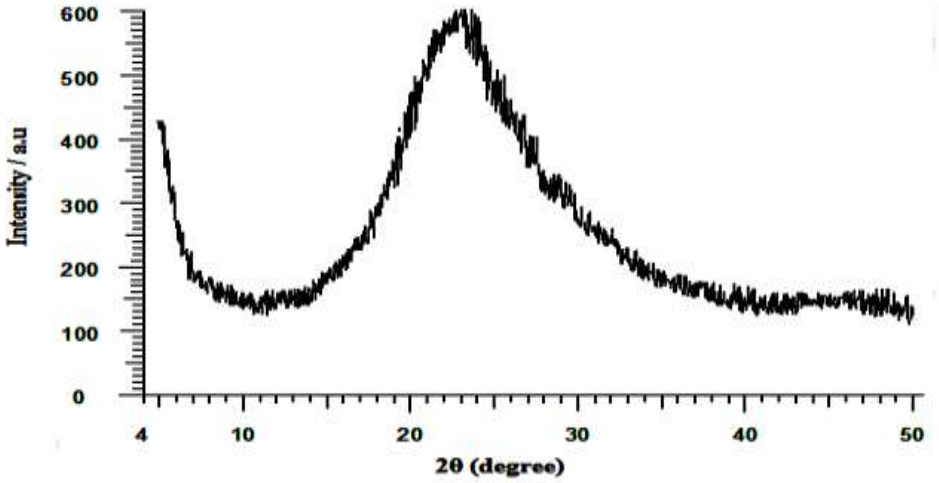

Figure 1. XRD image of silica extracted from BGA

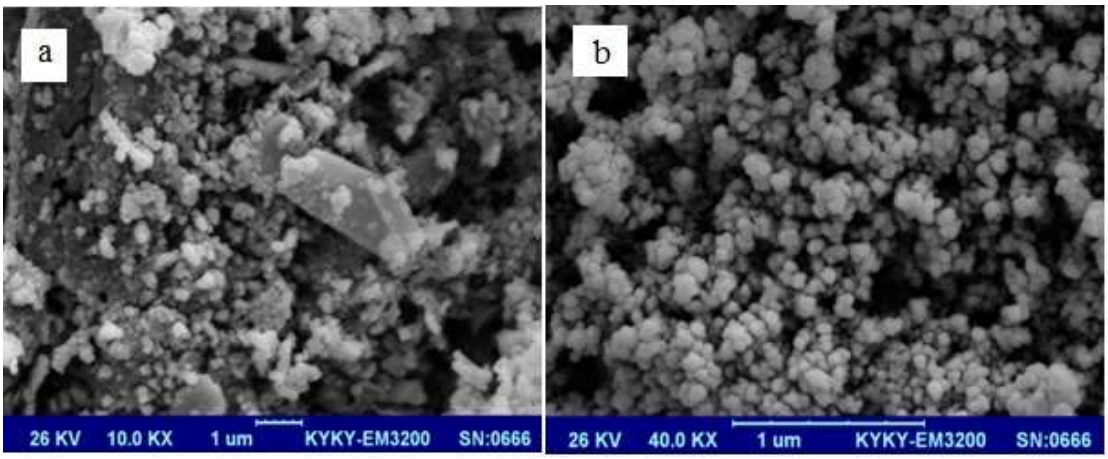

Figure 2. SEM images of (a) BGA white ash and (b) silica extracted from BGA

a) Effect of concentration of NaOH solution and temperature on the S/N ratio in both groups of responses

As Figures (3, 4 A) and (3, 4 B) show, the distribution of adsorbate between adsorbent and solution of Pb^{2+} and also values of extracted silicon by alkaline treatment are affected by concentration of NaOH solution and temperature. The results show that the concentration of

NaOH solution required for both responses is 0.2 M (level 2) that is confirmed according to references [16, 38-39]. Increasing the NaOH molarity from 0.1 to 0.2 led to increase in the S/N ratios from 37.9 to 38.6 and 44.3 to 46.3 for both responses, respectively. This trend is quite rational; the more is the alkalinity of the basic solution, the stronger is the chemical attack (hydrolysis) of the hydroxyl groups to the zeolite framework leading to the extraction and dissolution of the siliconoxide building blocks. But with the continuation of the trend in molarity 0.5, due to high concentration, it may demolish zeolite structure and result in decreasing the S/N ratio (37.9).

Also, the S/N ratio of both of the responses is increased up to level 2 (0.2 M and 55 Cº for concentration of NaOH solution and temperature, respectively). S/N ratio for the RP% Pb^{2+} and amount of extracted silicon at level 2 of these factors are 38.6, 38.4 and 46.8 and 46.6, respectively. With increasing temperature from 25 to 55Cº, S/N ratios increase from 38.2 to 38.4 and 45.6 to 46.6 for the first and the second responses which are in agreement with reported work over ZSM-5 [40]. Also, increasing temperature to 85 Cº, may cause destruction and degradation of the zeolite structure with exit silicon and result in meso pore more than 20 nm or macro pores. Then S/N ratio decreases from 38.0 to 38.2 and 46.6 to 45.

This result is in good agreement with the observation of Groen et al who studied the effect of temperature on desilication of parent H-ZSM-5. They suggested that meso-pores with a broad distribution size of 3-10 nm at temperature lower than 55 Cº and another group of mesopores centered at 10 nm were acquired in the ZSM-5 treated at 65 Cº, and additional mesopores were created in the same ZSM-5 at 20 nm by a treatment at a temperature higher than 75 Cº. It seemed that the mesopore size and volume were tuneful to a specific range [40]. Also, Abello et al, recently, used microwave as a heating source for alkaline treatment. They concluded that for mesopore formation, the treatment temperature is chemically efficient to intensify the rate of desilication of the zeolite framework [41].

b) Effect of time of reflux on the S/N ratio in both of responses

Figures (3, 4C) display the effect of time of reflux on the S/N ratio of the RP% Pb^{+2} and amount of extracted silicone, respectively. It is demonstrated that the S/N ratio of both of the responses increased continuously by varying the time of reflux. It is mentioned that S/N ratio for the RP% Pb^{+2} and amount of extracted silicon at maximum level (level3=2h) are 38.3 and 46.3, respectively. By increasing reflux time from 30 to 60 min, S/N ratios will increase from 38 to 38.2 and 44.9 to 46 for first and second response, respectively. This trend is rational. Also, with increasing time of reflux to 120 min, S/N ratios increase. In fact, as time increases, silicon has more opportunity for exiting from/through the zeolite structure.

c) Effect of molar ratio of TMAOH / NaOH on the S/N ratio (in both of responses)

The effect molar ratio of TMAOH / NaOH on the S/N ratio the RP% Pb^{2+} and amount of extracted silicon is shown in Figures (3, 4D). It is illustrated that the S/N ratio of desilication of parent H-ZSM-5 by TMAOH /NaOH (AT-ZSM-5) ratio= 0.5 is higher than that of samples treated with TMAOH /NaOH mixture with ratio 1.5. Less spacious

desilication of zeolite in the presence of TMAOH is devoted to its protective effect on zeolite structure resulting from the known affinity of TMA^+ cations to the zeolite surface. This is attributed to the adsorption of TMA^+ onto the zeolite sealing off most of the available external surface–and against what occurs in TMAOH /NaOH mixture with ratio 1.5[38]. In other words, tetra-alkyl-ammonium cations (TMA^+) are not strongly solvated in aqueous solution because of their larger effective cationic diameter. (e.g TMA^+ ca.0.6 nm, and the hydrophobicity of their alkyl groups, bringing about the attraction of less water molecules. This can be proved by the lower hydration enthalpy of tetra-alkyl-ammonium cations (ca. 135 kJ mol^{-1}) with respect to Na^+ (406 kJ /mol) tending to make the former cation less soluble [42]. The hydrophobicity of the TMA^+ causes methyl groups to interact with the hydrophobic silicate species rather than with the polar water molecules. Both arguments likely make the somewhat TMA^+ cation being more stable on the zeolite surface. As a result, in the presence of tetra-alkyl-ammonium cations, the zeolite surface is better shielded from the attack by OH^- with respect to sodium cations. The higher affinity of TMA^+ for the zeolite combined with its internal steric hindrance slows down the kinetics of the desilication process [43]. Also, the higher PR% can be distributed to a mesopore secondary pore system in order to facilitate the access to and diffusion within microporous zeolites. S/N ratio for the RP% Pb^{2+} and amount of extracted silicon at level 3 is 38.3 and 46.3, respectively.

Analysis of variance

According to the ANOVA results for removal of Pb^{2+} % in Table 4, the value A has the largest variance while other factors have less significant effects on removal of Pb^{2+} %. The degree of freedom (D.F.) for each factor was 2 and the total D.F. was 8. The variance for the error expression could not be achieved. Because the D.F. for the error expression was 0, it was impossible to calculate the F ratio as in a following Equation (3):

$$\boldsymbol{F\ ratio} = \frac{\boldsymbol{V}}{\boldsymbol{V_e}} \qquad (3)$$

Where v is variance v_e is variance for the error term. When sum of squares of each factor is less than 10% of sum of squares of the most effective factor, it can be disregarded. This process is named pooling, and the ignored factor is named pooled [44]. Therefore in this study, factor C (time of reflux) and D (molar ratio of TMAOH / NaOH), can be pooled. In order to remove the zero D.F. from the error expression, a pooled ANOVA is applied [45]. In this situation, the D.F. for error expression will be 4. The values of F-ratio were calculated after pooling the factors C and D which are given in Table 5. With considering the pooled ANOVA results, a (concentration of NaOH solution), has the largest variance on the removal of Pb^{2+} %. Hence A is the most important factor affecting the PR%. The higher removal of Pb^{2+} % can probably be assigned to a mesopore secondary pore system to facilitate the access to and diffusion of microporous zeolites. Less spacious desilication of high-silica zeolites in the presence of TMAOH is dedicated to its protective influence on zeolite structure, resulting from the known affiliation of TMA^+ cations to the zeolite surface. Also, the amounts of aluminum leached from the high-silica zeolite treated with a molar ratio TMAOH / NaOH = 0.5 are higher than that of samples treated with molar ratio TMAOH / NaOH =1.5. This is attributed to the same reason interpreted in above [38]. According to the

ANOVA results for the amount of extracted silicon in Table 6, the value A has the largest variance while other factors have less significant effects on the amount of extracted silicon. Likewise, the degree of freedom (D.F.) for each factor was 2 and the total D.F. was 8. The variance for the error expression could not be achieved because the D.F. for the error expression was 0. Factor D (molar ratio of TMAOH/ NaOH), can be pooled. Table7 is named a pooled table because the factors that do not have significant effect on the amount of extracted silicon left out. In this situation, the D.F. for error expression will be 2. The values of F-ratio were calculated after pooling the factor D, given in Table 7. Considering the pooled ANOVA results, A (concentration of NaOH) has the largest variance on the amount of extracted silicon. Therefore, A is the most important effective factor on the amount of extracted silicon. Realizing the interaction between each of the two factors admitted a better insight into the entirely process analysis. Any one factor may interact with ther factors creating the eventuality to attain a great number of interactions. In this way, the estimated interaction named the severity index (SI) of the different factors under perusal helped understanding of the influence of the two individual factors at diverse levels of the interactions [46]. In (Table 8a, b), the "columns" indicate the positions to which the interacting factors were defined. The "reserved" column displays the column that should be reserved if the effect of this special interaction is to be studied. "Levels" illustrate the factor levels favorable for the optimum conditions (based on the first two levels). From (Table 8a, b), A (concentration of NaOH solution) and D (molar ratio of TMAOH / NaOH) showed highest SI (48.15%) followed B (temperature) and D (molar ratio of TMAOH / NaOH) SI (44.31%) etc. for the removal of Pb^{+2} %. Similarly, B (temperature) and D (molar ratio of TMAOH / NaOH) which displayed highest SI (66.17%) followed A (concentration of NaOH) and D (molar ratio of TMAOH / NaOH) which, in turn, showed highest SI (51.62%) for the amount of extracted silicon.

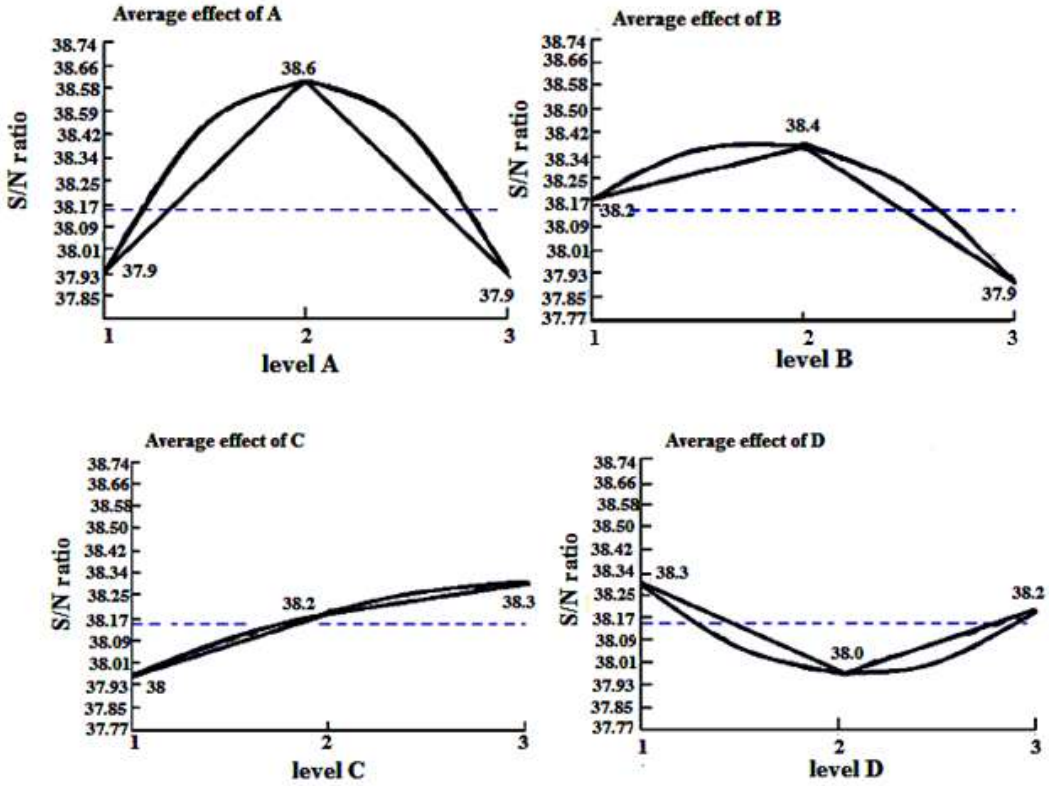

Figure 3. Main effects of factors (by S/N ratio) for PR% Pb^{2+}

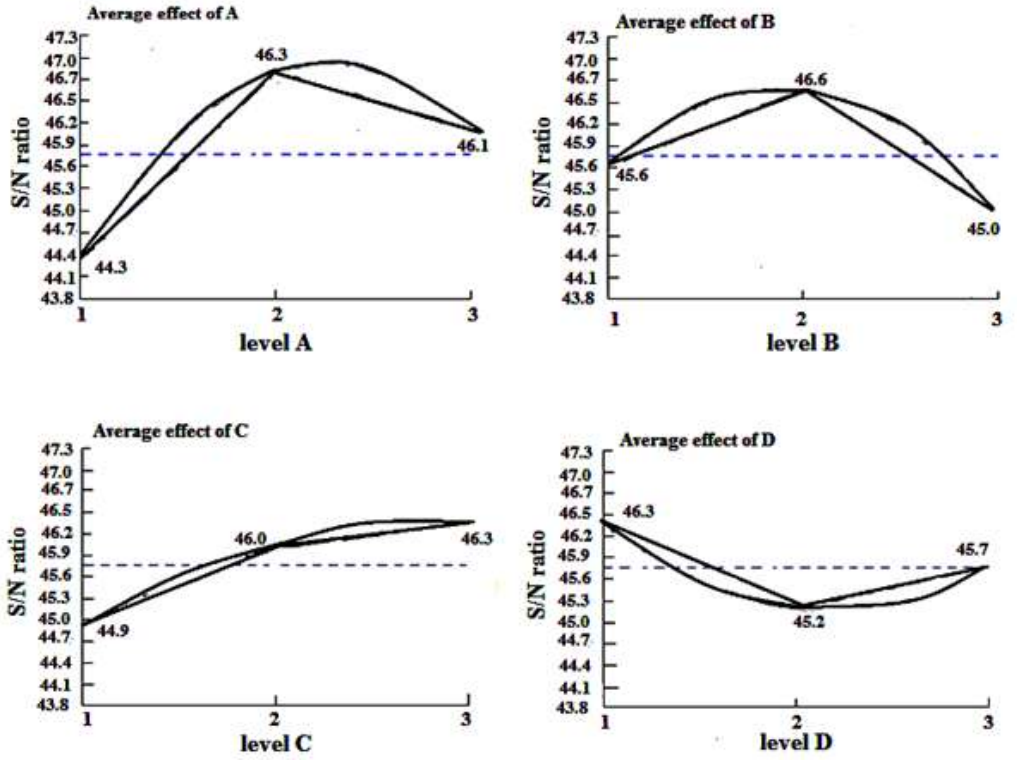

Figure 4. Main effects of factors (by S/N ratio) for amount of extracted silicon

Table 4. ANOVA analysis of signal-to-noise ratio (S/N) for removal of Pb^{+2} %

Factor	Degree Of Freedom (DOF)	Sum of Squares(S.S.)	Variance (V)	F-Ratio (F)	Pure Sum (S)	Percent P(%)
A	2	0.889	0.449	-	0.889	58.195
B	2	0.312	0.156	-	0.312	20.224
C	2	0.173	0.086	-	0.173	11.24
D	2	0.159	0.079	-	0.159	10.332
Other/Error						
Total	8	1.545				100.**00**%

Table 5. Pooled ANOVA analysis of signal-to-noise ratio (S/N) for removal of Pb^{+2} %

Factor	Degree Of Freedom (DOF)	Sum of Squares(S.S.)	Variance (V)	F-Ratio (F)	Pure Sum (S)	Percent P(%)
A	2	0.906	0.453	5.415	0.739	47.636
B	2	0.311	0.155	1.858	0.143	9.266
C	(2)	(0.168)		pooled		
D	(2)	(0.166)		pooled		
Other/Error	4	0.334	0.083			43.098
Total	8	1.552				1**00**%

Table 6. ANOVA analysis of signal-to-noise ratio (S/N) for the amount of extracted silicon

Factor	Degree Of Freedom (D.F.)	Sum of Squares(S.S.)	Variance (V)	F-Ratio (F)	Pure Sum (S)	Percent P(%)
A	2	9.958	4.979	-	9.958	52.214
B	2	4.057	2.028	-	4.057	21.272
C	2	3.144	1.572	-	3.144	16.484
D	2	1.911	0.955	-	1.911	10.021
Other/Error	0					
Total	8	19.072				100.**00**%

Table 7. Pooled ANOVA analysis of signal-to-noise ratio (S/N) for the amount of extracted silicon

Factor	Degree Of Freedom (D.F.)	Sum of Squares(S.S.)	Variance (V)	F-Ratio (F)	Pure Sum (S)	Percent P(%)
A	2	9.958	4.979	5.21	8.047	42.193
B	2	4.057	2.028	2.122	2.145	11.251
C	2	3.144	1.572	1.645	1.232	6.463
D	(2)	(1.911)		pooled	CL=+NC+	
Other/Error	2	1.912				40.093
Total	8	19.072				100.**00**%

Table 8. Estimated interactions of severity index for two factors in a) removal of Pb^{2+} % b) the amount of extracted silicon

a)

≠	Interacting Factor pairs (Order based on SI)	Columns	SI (%)	Reserved col	Levels
1	A × D	1 × 4	48.15	5	[2,1]
2	B × D	2 × 4	44.31	6	[2,1]
3	B × C	2 × 3	30.79	1	[2,3]
4	A × C	1 × 3	25.5	2	[2,3]
5	A × B	1 × 2	12.51	3	[2,2]
6	C × D	3 × 4	2.9	7	[3,1]

b)

≠	Interacting Factor pairs (Order based on SI)	Columns	SI (%)	Reserved col	Levels
1	B× D	2 × 4	60.83	6	[2,1]
2	A × D	1 × 4	51.51	5	[2,1]
3	B × C	2 × 3	41.76	1	[2,3]
4	C × D	3 × 4	20.59	7	[3,1]
5	A × C	1 × 3	12.08	2	[2,3]
6	A × B	1 × 2	10.86	3	[2,2]

Optimum levels and estimation of optimum response characteristics

The optimized parameters for both of responses obtained from the statistical software are listed in Table 9 which summarizes the optimum conditions and the predicted and actual experimental values. According to Table9, at optimum condition, the first level of D (molar ratio of TMAOH / NaOH), second level of the A (concentration of NaOH), B (temperature) and third level of C (time of reflux) in the AT-ZSM-5 of both of responses, removal of Pb^{2+} and amount of extracted silicon suggest that they have the average values of *S/N* ratio (= 39.097), (=48.878) despite that of other levels, respectively. At optimum levels of the process factors, one confirmation experiment with three times reproducible (on AT-05-ZSM-5) was carried out for percentage of removal of Pb^{2+} and amount of extracted silicon. As can be seen in Table9, both of the responses in the case of expected and confirmatory experiments are in good agreement with each other at optimum condition and it should be considered that inside the marked range of process factors (with 90% of confidence level) , these optimum values are logical and valid. Concerning the factors utilized in this work at optimum condition, the maximum percentage of removal of Pb^{+2} and value extracted silicon in actual values are 90.2 and 278.13 mg /L, respectively.

Table 9. Optimum and confirmative values of the process parameters for maximum Responses to resulting higher average values of S/N 39.097, 48.878 for Removal of Pb^{+2}% and amount of extracted silicon (mg L^{-1})

Optimal levels of process parameters	Predicted optimal responses		Average of confirmation experiments	
	Removal of Pb^{+2}%	Extracted Si(mg L^{-1})	Removal of Pb^{+2}%	Extracted Si(mg L^{-1})
A: concentration of NaOH= 0.2 M B: temperature= 55 C° C: time of reflux= 100 min D: (molar ratio TMAOH / NaOH) = 0.5	90.15	278	90.20	278.13

Physicochemical properties of the parent and AT-05-ZSM-5 zeolites

XRD patterns

XRD patterns of the parent H-ZSM-5 were synthesized and AT-05-ZSM-5 zeolites were shown in Figure 5a, b. The main peaks at 2θ = 7.9, 8.9, 23.2 and 24.5º are related to ZSM-5 [49]. For investigating the possible structural changes in the parent H-ZSM-5 zeolite after AT, XRD analysis was performed. Parent H-ZSM-5and AT-05-ZSM-5 displayed XRD peaks at similar positions. No peak from impurities appeared. These patterns of ZSM-5 have shown good crystallinity and the intrinsic MFI structure was preserved. Moreover, no additional phase was formed and crystal structure was not destroyed during the alkaline treatment. However, the XRD pattern of AT-05-ZSM-5 has shown broader peaks with lower intensities than that of parent H-ZSM which indicates that the crystallinity or the nominal crystal size was effectively reduced and increased specific surface area. This can be explained by the occurrence of hydroxide anion from the NaOH solution attacking the silanol groups and Si-O-Si or Si-O-Al bonds causing damage to the crystal structure. In spite of the fact that the alkaline treatment of the zeolite is accompanied by a preference removal of siliceous species, the results verified that desilication by alkaline treatment of Parent H-ZSM-5practically did not disturb the long-range crystallinity of the resulting materials. An eventual explanation for these observations is that little amount of crystalline or amorphous phase material in the parent H-ZSM-5 is particularly removed by alkali solutions without significant destruction of the zeolite MFI framework [39]. Because of over that of framework Al in the alkaline medium, the dissolution of framework Si is preferred over that of framework Al in the alkaline medium. This can be related to the fact that the negative charge of AlO_4^- tetrahedral in the ZSM-5 framework prevents the extraction of Al through hydrolysis of Si–O–Al bonds by negatively charged hydroxyl ions. In addition, it is generally approved that the presence of AlO_4^- protects the neighboring Si atoms against OH^- attack [47]. Hence, a preferential removal of siliceous species occurred during the desilication parent H-ZSM-5 with Si/Al=35.

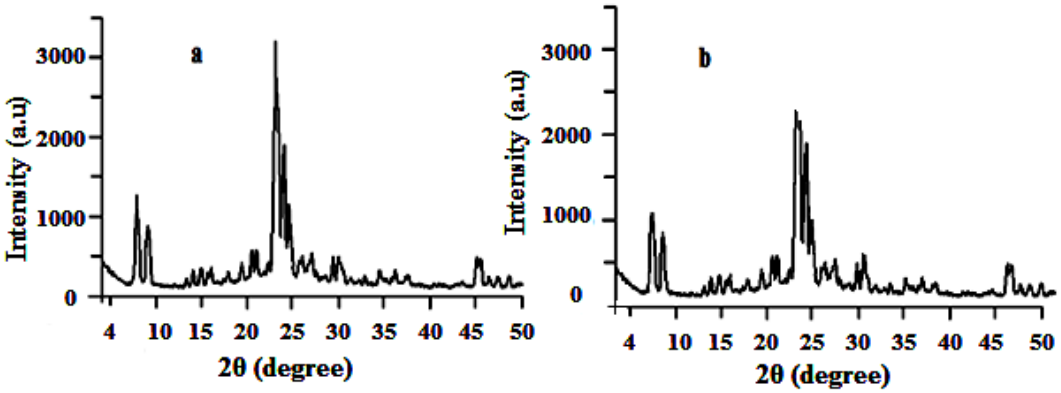

Figure 5. X-ray diffraction patterns a) parent H-ZSM-5 b) AT-05-ZSM-5

ICP-OES analysis

According to Table 10, the analysis of filtrates by ICP-OES approved the higher amount of Si was leached during the treatment in AT-05-ZSM-5 (278 mg /L) in comparison to the treatment in other AT-ZSM-5. Less extensive desilication of parent H-ZSM-5 in the presence of TMAOH is distributed to its protective effect on zeolite structure resulting from the known affinity of TMA^+ cations to the zeolite surface. The amounts of aluminum leached in AT-08-ZSM-5 (1.820 mg /L) were higher than that of other treated samples in Table10. This is attributed to the adsorption of TMA^+ onto the zeolite which is sealing off most of the available external surface, that would largely prevent surface realumination in opposition to what occurs in AT-05-ZSM-5 and in another AT-ZSM-5 that have less TMAOH concentration in molar ratio of TMAOH / NaOH. This suggests that not all the Al removed from the framework during the alkaline treatment remains in the liquid phase, but is in some manner re-incorporated in the solid. Significantly, when the pH decreases due to consumption of OH^- ions during the alkaline treatment the solubility of Al decreases and deposition is advanced [48]. For zeolites with a molar Si/Al ratio in the range 25-50, a decrease is typically observed from pH 13.3 to 12.2 which indicates that more than 90% of the initial OH^- ions have been consumed. Deposition of Al species during the alkaline treatment is further confirmed by the observations [4,40] that the Al concentration in the filtrate decreases in what time the duration of the alkaline treatment is increased while the Si concentration increases increasingly [48]. Hence, the formation of meso-pores in the nanometer size range (Figure 7a, b and 8a, b) with a large meso-pore volume claims to removal of both framework of Si and framework of Al essentially. Scheme 1 demonstrates desilication by AT on parent H-ZSM-5 (Si/Al=35).

Table10. Chemical composition filtrated solutions related to parent H-ZSM-5 and AT-ZSM-5

parent H-ZSM-5A	Si filtered (mg L^{-1})	Al filtered(mg L^{-1})	Si/Al
[a]AT-[b]01-ZSM-5	158	0.240	658.33
AT-02-ZSM-5	176	0.238	739.495
AT-03-ZSM-5	161	0.210	766.66
AT-04-ZSM-5	220	0.281	782.91
AT-05-ZSM-5	278	0.283	982.33
AT-06-ZSM-5	172	0.350	491.428
AT-07-ZSM-5	199	0.520	382.69
AT-08-ZSM-5	201	1.820	110.43
AT-09-ZSM-5	203	0.321	632.39

[a]Alkaline treatment
[b]number of experiments

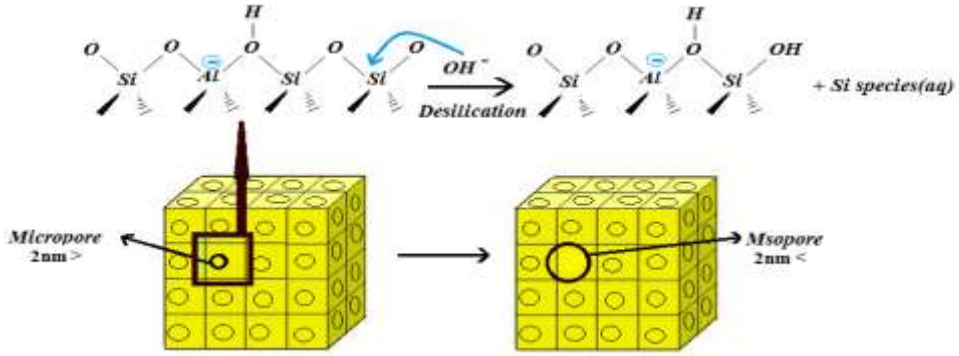

Scheme 1. desilication by alkaline treatment onparent H-ZSM-5(Si/Al=35)

FT-IR spectrum

In Figure 6, FT-IR parent H-ZSM-5 and AT-05-ZSM-5 spectrums of the samples which show the bands around 792, 1080-1220 cm^{-1} are characteristic of SiO_4 tetrahedron units. The difference between ZSM-5 zeolite and other type of zeolites is marked from the absorption bands at 1219 and 540 $cm^{-1.}$ The external asymmetric stretching vibration near 1220 cm^{-1} gives information on the presence of structures containing four chains of five-member rings of ZSM-5 structure. The band near 792 cm^{-1} is attributed to the symmetric stretching of external linkages and the one near 540 cm^{-1} is assigned to a structure-sensitive vibration caused by the double five-member rings of the external linkages. The absorption band near 450 $cm^{-1}$is due to the TeO bending vibrations of SiO_4 and AlO_4 internal tetrahedral. The presence of absorption bands around 540 and 450 $cm^{-1}$are characteristic of the ZSM-5 crystalline structure [49]. In Figure 6, FT-IR parent H-ZSM-5 and AT-05-ZSM-5 spectrums were displayed in OH stretching area (3400-4000). According to literature [47], the parent sample H-ZSM-5 displays two bands, the bands at around 3610 $cm^{-1}$is assigned to the framework bridged hydroxyl groups(Al(OH)Si) while that at around 3700–3740 cm^{-1} it is specified with $SiOH(SiO)_3$, i.e. separated silanol groups at the external surface, free silanol and internal silanol groups of defect sites. The intensity of the band around 3700–3740 cm^{-1}, after alkaline treatment, increases representing the raises of $SiOH\ (SiO)_3$ concentration. As shown in Figure 6, treated sample demonstrated a band of OH groups

connected to extra framework Al at 3670cm^{-1} which is shifted by alkali metal ion from 3660cm^{-1}to 3670cm^{-1} [50]. Moreover, it was also found that the intensity of the band at 3745cm^{-1} is usually the characteristic of terminal Si–OH groups. In parent H-ZSM-5 – due to large crystals and low meso-pore surface area – any absorption band in 3745 cm^{-1}was not displayed until the desilication was brought by terminal Si–OH groups 3745 cm^{-1} that was in turn resulted from inserted mesopores in alkaline treatment [51]. The absorption band at 3610 cm^{-1}, which is characteristic of bronsted acid sites, was slowly increased because of extraction extended silicon from zeolite structure and raising Aluminum value [14].

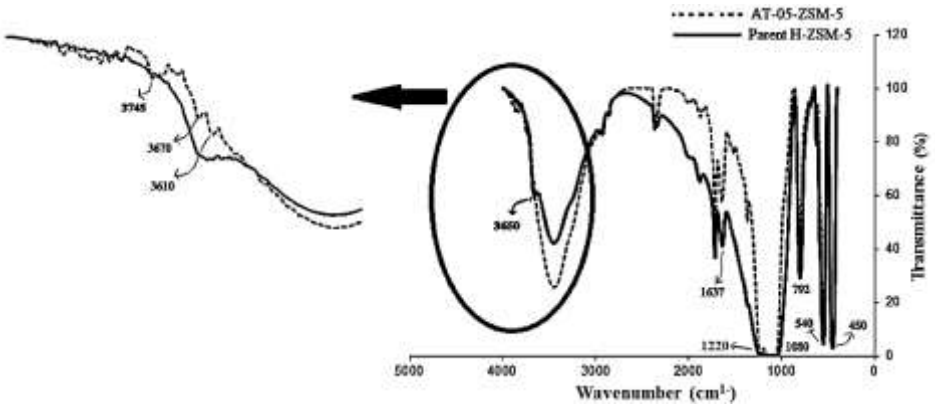

Figure 6. FT-IR spectra of the parent H-ZSM-5(———) and AT-05-ZSM-5(- - - -)

BET and BJH isotherms

According to the literatures [52, 53], the removal of silicon species from the zeolites cause changes in their pores volumes, pores size distribution and specifics surface area. Figure 7a, b and 8a, b show the N_2 adsorption and desorption isotherms (BET) and the corresponding BJH pore size distribution (PSD) curves at 77.3 K for the parent H-ZSM-5 and AT-05-ZSM-5. Table11 displays textural properties of parent H-ZSM-5 and AT-05- ZSM-5. As seen from Figure 7a, b, the nitrogen isotherms of the parent H-ZSM-5 demonstrates only a typical type-I isotherm, confirming its microporous character without considerable meso-porosity that is confirmed by its BJH pore size distribution curve Figure 8a, b. As reported in Table11, the BET total pore volume and surface area of parent H-ZSM-5 are 0.183 cc /g and 352 m^2 /g, but at the similar time as the pore volume mesoporous and surface area are 0.075 cc/g and 21 m2 /g, respectively. Moreover, the BET total pore volume and surface area of AT-05-ZSM-5 are 0.362 cc /g and 401 m^2 /g, while the pore volume mesoporous and surface area are 0.324 cc /g and 389 m^2 / g^{-1}, respectively. Also, alkaline treatment of ZSM5 zeolite leads to an isotherm indicating the type IV with a considerably enhanced uptake of nitrogen at higher pressures p/p_0 =0.4 attached by a hysteresis loop. This proposes the presence of both micro and meso-porosity (hierarchical porous system) as reported by van Laak *et al*. [54] and Wang *et al*. [55] As can be seen in Figure 8a, b, the pore size distribution is centered at about 1.69 nm which specifies the microporous nature of parent H-ZSM-5. Also, AT-05-ZSM-5 demonstrates a limit and uniform meso-pore average size distribution at 7.65 nm.

Table 11. Textural properties of the parent and alkaline-treated ZSM-5 samples

Sample	Pore volume (cc g^{-1})			Surface area (m^2 g^{-1})		
	[a]V_{total}	[b]V_{micro}	[c]V_{meso}	[d]S_{BET}	[e]S_{micro}	[f]S_{meso}
Parent H-ZSM-5	0.183	0.108	0.075	352	331	21
AT-05-ZSM-5	0.362	0.038	0.324	401	12	389

[a]Total pore volume at p/p_0=0.99
[b]Micropore volume calculated by the t-plot method
[c]Mesopore volume calculated by $V_{total} - V_{micro}$
[d]BET surface area
[e]Micropore surface area evaluated by t-plot method
[f]Mesopore surface area calculated using S_{BET} - S_{Micro}

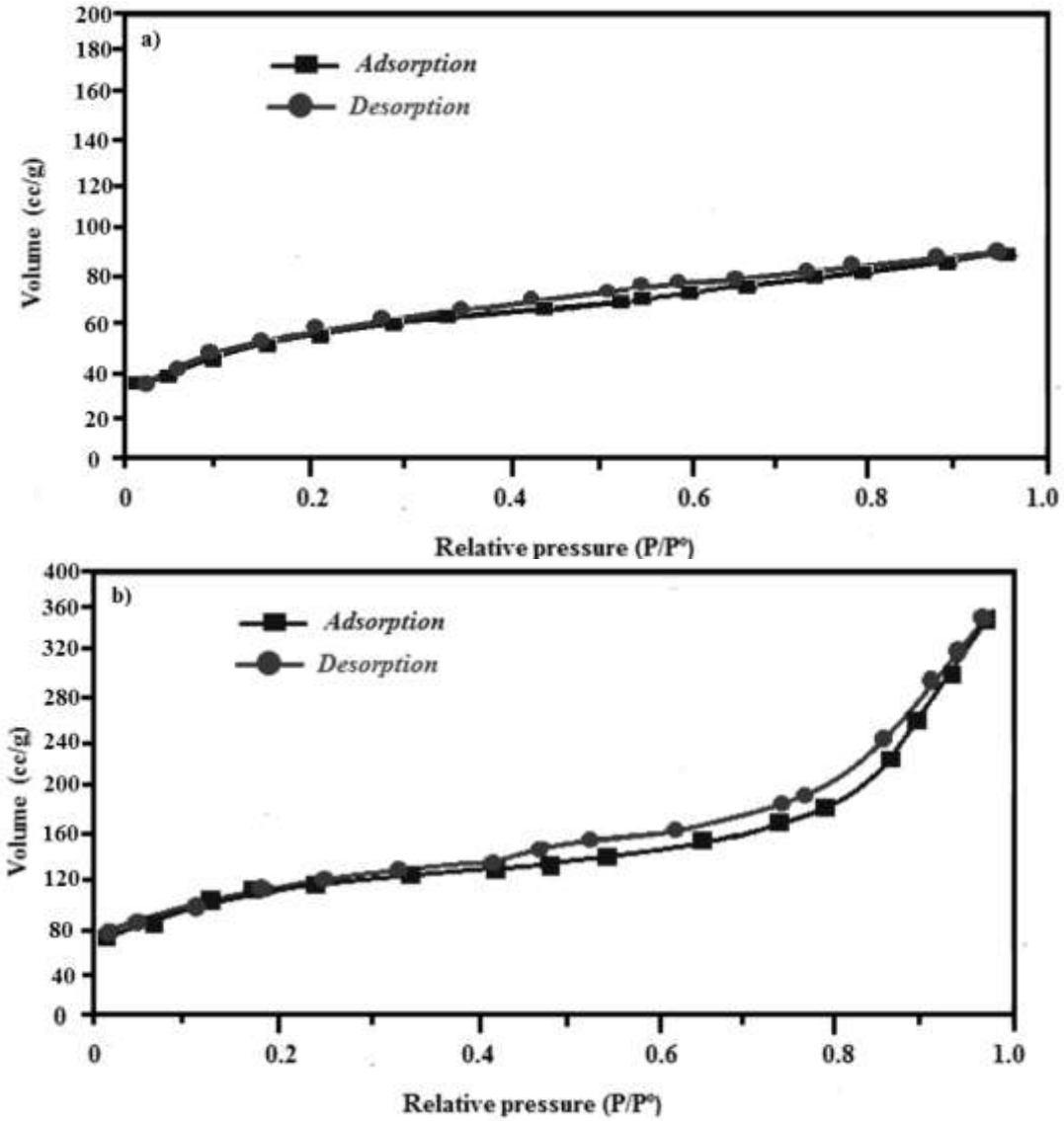

Figure 7. N_2 adsorption-desorption isotherms of the a) parent H-ZSM-5 and b) AT-05-ZSM 5samples

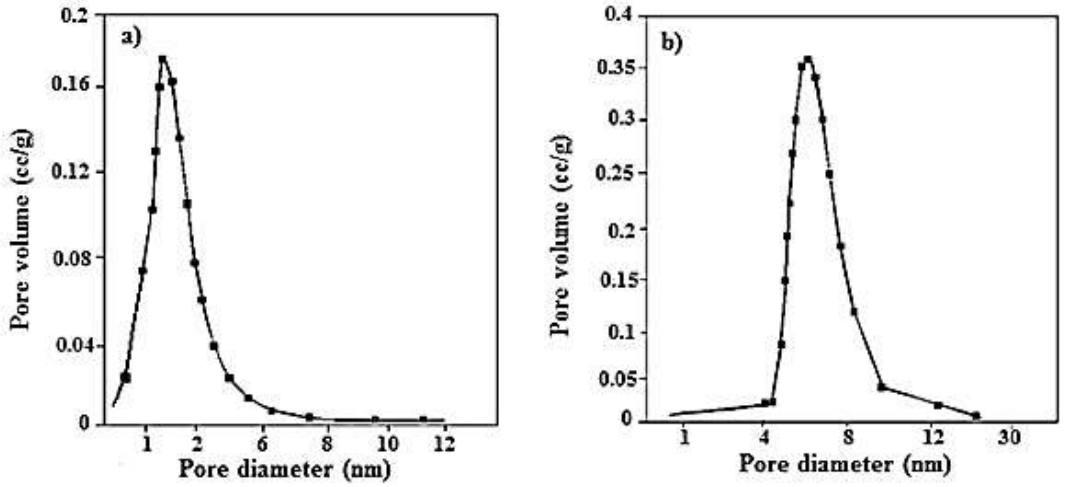

Figure 8. BJH pore size distribution curves of the a) parent H-ZSM-5 and b) AT-05-ZSM-5

SEM images

In Figures 9 (a, b), 10(a, b and c), The SEM micrographs of the parent H-ZSM-5 and AT-ZSM-5 are shown. As apparently displayed in Figure 9 (a, b), the crystals size of the parent H-ZSM-5 is large, and their surfaces are completely smooth which verifies the absence of mesopores in its structure. But the post-alkaline treatment makes a considerable change in the surface and morphology of the parent H-ZSM-5. Slits, gaps and cracks appeared on the surface of crystal. Anyway, the overall crystal size does not change much during treatment. As seen in Figure 10 (a, b and c), average size distribution at 7.65nm related to AT-05-ZSM-5 was confirmed by SEM. As shown in Figure 9 (a, b), 10(a, b and c), the sample treated with a TMAOH/NaOH mixture (R = 0.5) in fifth experiment displays more similar intra-crystalline meso-pores that span through the entire surface of the parent H-ZSM-5 crystal. Besides, being conserved, the crystal shape represents the removal of silicon species correctly. The supplemented meso-porosity is probably the main cause for the facilitation and maximum adsorption of lead ions to micro-pores. In fact, AT-05-ZSM-5 could have had the role of both adsorption and catalytic roles.

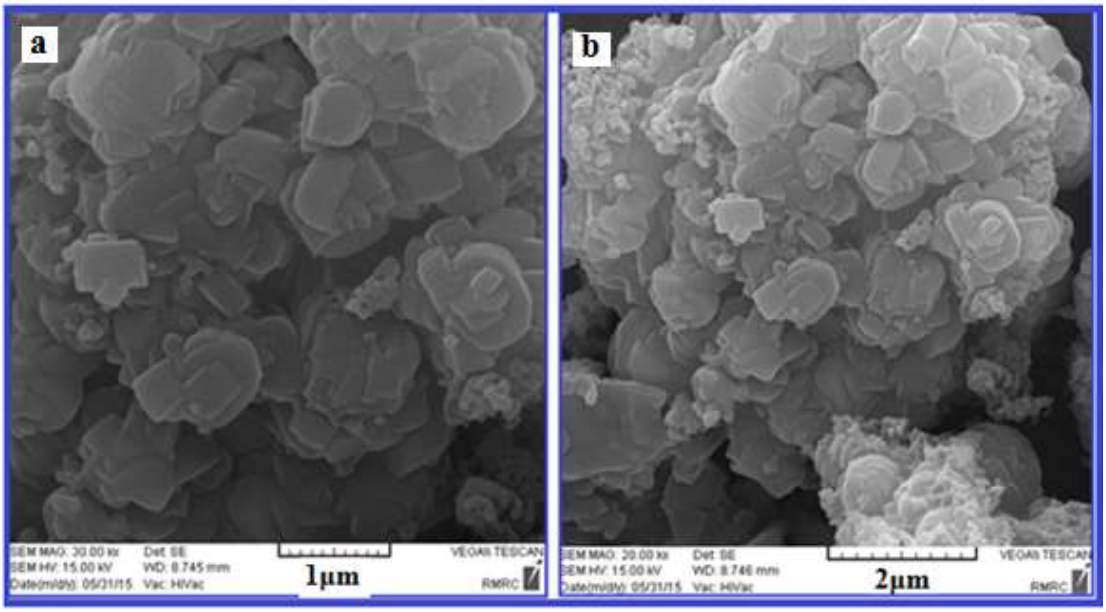

Figure 9. SEM images of a) 1µm b) 2µm parent H-ZSM-5 before desilication by alkaline treatment

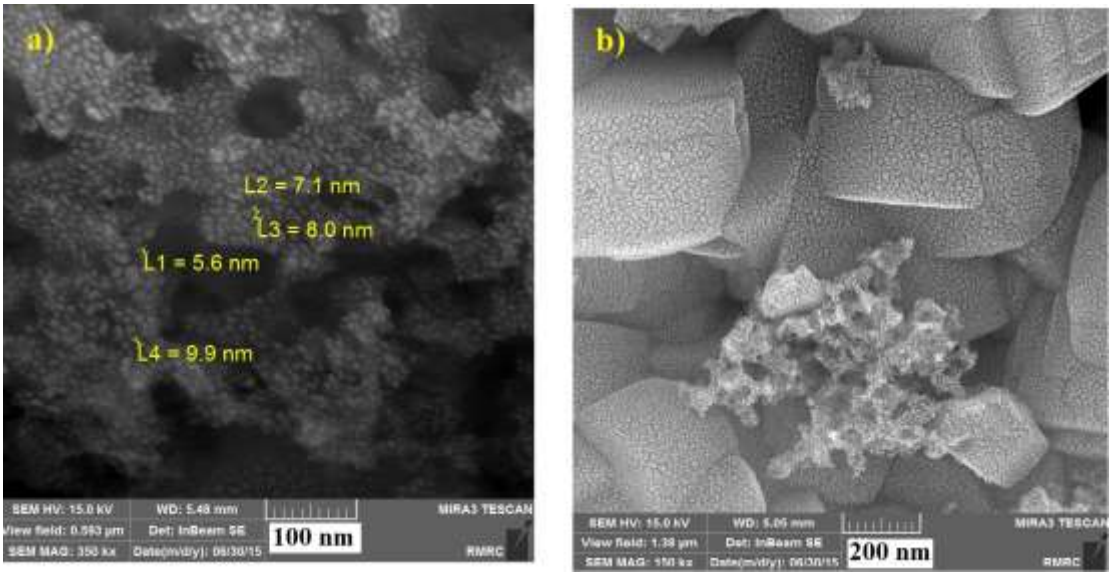

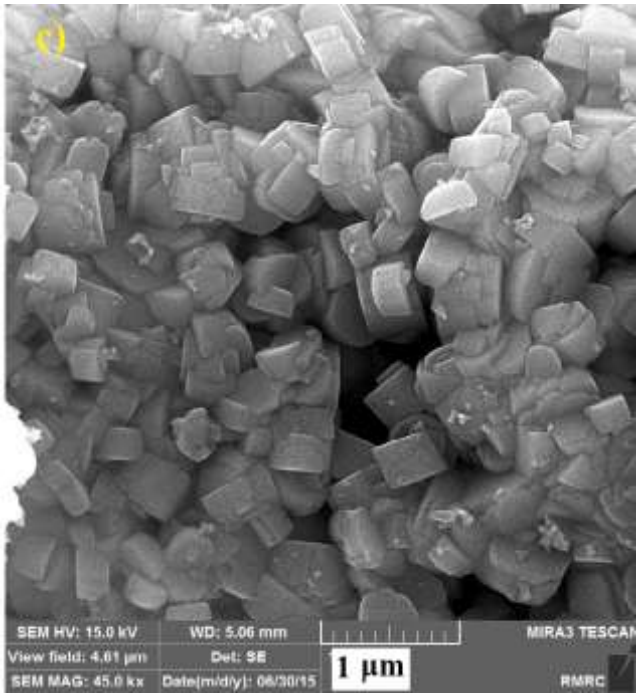

Figure 10. SEM images of a) 100nm b) 200nm c) 1µm parent H-ZSM-5 after desilication by alkaline treatment (AT-05-ZSM-5)

Conclusion

In this study, at first, silica was extracted from BGA ash, and then it was used for synthesizing the nanoporous parent H-ZSM-5 zeolite by hydrothermal method. Then, post-synthetic modification of parent H-ZSM-5 zeolite (Si/Al=35) was investigated by desilication of alkaline treatment using mixed NaOH and TMAOH for preparing hierarchical H-ZSM-5 zeolite applying Taguchi method. The optimum conditions for both responses amount of the extracted silicon and removal of Pb^{2+} % from aqueous solutions were determined by the Taguchi Method as; (A) Concentration of NaOH solution=0.2 M, (B) temperature =55 C°, (C) time of reflux=120 min and (D) molar ratio of TMAOH /NaOH =0.5. Also, the results displayed that in comparison with other factors, Concentration of NaOH solution was the most effective one in both responses. According to the results, AT-05-ZSM-5 (05=fifth run) is the optimum and appropriate zeolite for the amount of extracted silica (278.13 mg /L) and removal of Pb^{+2} % from aqueous solutions (90.2%) with *S/N* ratios (=48.878), (= 39.097), respectively. The characterization results reveal that the alkaline treatment of H- ZSM-5 zeolite leads to the formation of a hierarchical porosity with average size distribution at 7.65 nm. The analysis of filtrates by ICP-OES approved the higher amount of Si was leached during the treatment in AT-05-ZSM-5 (278 ppm) in comparison to the treatment in other AT-ZSM-5.

Acknowledgments

The authors would like to acknowledge the financial supports from University of Mazandaran.

References

[1] A.E.W. Beers, T.A. Nijhuis, F. Kapteijn, J.A. Moulijn, *Microporous Mesoporous Mater*., **2001**, *48*, 279-284.

[2] M.A. den Hollander, M. Wissink, M. Makkee, J.A. Moulijn, *Appl. Catal A.*, **2002**, *223*, 85-102.
[3] J. Perez-Ramirez, F. Kapteijn, G. Mul, J.A. Moulijn, *J. Catal.*, **2002**, *207*, 113-126.
[4] M. Ogura, SY. Shinomiya, J. Tateno, Y. Nara, M. Nomura, E. Kikuchi, M. Matsukata, *Catal A.*, **2001**, *219*, 33-43.
[5] J. Perez-Ramirez, F. Kapteijn, J.C. Groen, A. Doménech, G. Mul, J.A. Moulij, *J. Catal.*, **2003**, *214*, 33-45.
[6] X. Zhao, G.Q. Lu, G.J. Millar, *Ind. Eng. Chem. Res.*, **1996**, *35*, 2075-2090.
[7] J.C. Groen, A.A. Louk Peffer, J. Perez-Ramirez, *Microporous and Mesoporous Mater*., **2003**, *60*, 1-17.
[8] W. Guo, L. Huang, P. Deng, Z. Xue, Q. Li, *Microporous Mesoporous Mater.*, **2001**, *427*, 44-45.
[9] M.T. Janicke, C.C. Landry, S.C. Christiansen, S. Birtalan, G.D. Stucky, B.F. Chmelka, *Chem. Mater.*, **1999**, *11*, 1342-1351.
[10] H.R. Liu, X.C. Meng, D.S. Zhao, Y.D. Li, *Chem. sEur. J.*, **2008**, *140*, 424.
[11] H.J. Zhang, X.C. Meng, Y.D. Li, Y.S. Lin, *Ind. Eng. Chem Res.*, **2007**, *46*, 186-4192.
[12] H.F. Makki, *Int. J. Sci. tech.*, **2014**, *3*, 391-399.
[13] A. Eiemek, B. Subotic, R. Aiello, F. Crea, A. Nastro, C. Tuoto, A. Eiemek, B. Subtotic, I. Sumit, A. Tonejc, R. Aiello, F. Crea, A. Nastro, *Microporous Mater.*, **1995**, *4*, 159.
[14] T.S. Le, R**.** Le Van Mao, *Microporous Mesoporous Mater.*, **2000**, *34*, 93-97.
[15] J.C. Groen, L.A.A. Peffer, J.A. Moulijn, J. Perez-Ramirez, *Electrochimica Acta.*, **2014**, *147*, 279-287.
[16] F. Jin, Y. Tian and Y. Li, *Ind. Eng. Chem. Res.*, **2009**, *48*, 1873-1879.
[17] M. Yin, Z. Li, Z. Liu, X. Yang, and J. Ren, *ACS Appl. Mater. Interfaces*, **2012**, *4*, 431-437.
[18] F. Tadayon, S. Motahar, M. Hosseini, *Academic Research International*, **2012**, 242-48.
[19] K. Yetilmezsoya, S. Demirel, R.J. Vanderbei, J. *Hazard. Maters*, **2009**, *171*, 551-562.
[20] M.A.M. Khraisheh, Y.S. Al-degs, W.A.M. Mcminn, *Chem. Eng. J.*, **2004**, *99*, 177-184.
[21] T.A. Kurniawan, G.Y.S. Chan, W.H. Lo, S. Babel, *Sci. Total. Environ.*, **2006**, *366*, 409-426.
[22] O. Yavuz, Y. Altunkaynak, F. Guzel, *Water Res.*, **2003**, *379*, 48-952.
[23] A. Ahmadi, S. Heidarzadeh, A.R. Mokhtari, E. Darezereshki, H. Asadi Harouni, *J. Geochem. Explor*, **2014**, *147*, 151-158.
[24] M.R. Rezaei Kahkha, M. Kaykhaii, and G. Ebrahimzadeh, *Health Scope*, **2015**, 4e, 20667.
[25] H.R. Tashauoei, H. Movahedian Attar, M.M. Amin, M. Kamali, M. Nikaeen, M.A., *A, J. Environ. Sci. Tech.*, **2010**, *3*, 497-508.
[26] M.C. Silaghi Submitted on 6 Mar **2015**.TEZ.
[27] K.K. Tan and K.Z. Tang, *Eur. J. Operational Res.*, **2001**,*128*, 545-557.
[28] A.R. Khoei, I. Masters, and D.T. Gethin, *J. Materials Proce. Techn.*, **2002**, *27*, 96-106.
[29] J. Casab, D. Orsolya, L. Anna, A.Eya, N. Lstyan. J. Immunol, *J Immunol Method*, **2003**, *223*, 37-146.
[30] U. Kalapathy, A. Proctor, J. Shultz, *Bioresour.Technol*, **2000**, 732, 57-262.
[31] G. Zolfagharian, A. Esmaili-Sari, M. Anbia, H. Younesi, S. Amirmahmoodi, *J. Hazard. Mater*, **2011**, *192*, 1046-1055.
[32] G. Taguchi., McGraw-Hill, New York, USA, **1990**.

[33] A.R. Alao, Int. J. Precision Technology, **2011**, *2*, 1.
[34] H. Atil, Y. Unver, Biol., *Biol. Sci.*, **2000**, *3*, 1538-1540.
[35] J. Antony, *Qual. Realiab. ENG. Int.*, **2000**, *16*, 3-8.
[36] M. Kaneda, T. Tsubakiyama, A. Carlsson, Y. Sakamoto, T. Ohsuna, O. Terasaki, S.H. Joo, R. Ryoo, *J. Phys. Chem B*, **2002**, *106*, 1256-1266.
[37] E.P. Barret, L.G. Joyner, P.P. Halenda, *J. Am. Chem. Soc.*, **1951**,*73*, 373-380.
[38] J. Ahmadpour, M. Taghizadeh, *C.R. Chimie.*, **2015**, *18*, 834-847.
[39] S. Octaviani, Y.K. Krisnandi, I. Abdullah, and Riwandi Sihombing, *Makara Journal of Science*, **2012**, *16*, 155-162.
[40] J.C. Groen, L.A. A. Peffer, J.A. Moulijn, Perez-Ramirez, *Colloids and Surfaces A: Physicochem. Eng. Aspects*, **2004**, *241*, 53-58.
[41] S. Abello, and J. Prez-Ramirez, *Phys.Chem.Chem.Phys*, **2009**, *11*, 2559.
[42] S. Abello, A. Bonilla, J. Perez-Ramırez, *Appl. CataL. A Gen., M.*, **2009**, *364*, 191-198
[43] M. M. Helmkamp and M. E. Davis, Annu. *Rev. Mater. Sci.*, **1995**, *25*, 161-92.
[44] M.A. Behnajady, M. Hajiahmadi, and N. Modirshahla, *Ind. Eng. Chem. Res.*, **2012**, *51*,15324-15330.
[45] J. Zolgharnein, N. Asanjarani, T. Shariatmanesh, *Int. Biodeter. Bioderg*, **2013**, *85*, 66-77
[46] S. N. Azizi & N.Asemi, *J. Environ. Sci. and Heal*, **2010**, *45*, 766-773.
[47] J. C. Groen, J. A. Moulijn and J. Perez-Ramirez, *J. Mater. Chem.*, **2006**, *16*, 2121-2131.
[48] J.C. Groen, L. A. A. Peffer, J. A. Moulijn, and J. Prermirez, *Chem. Eur. J.*, **2005**, *11*, 4983- 4994.
[49] J.B. Raoof, N. Azizi, R. Ojani, S. Ghodrati, M. Abrishamkar, F. Chekin, *Int. J. of hydrogen energ.*, **2011**, *36*, 13295 -13300.
[50] D. Tzoulaki, A. Jentys, J. Perez-Ramirez, K. Egeblad, *Catal. Today*, **2012**,*198*, 3-11.
[51] A. Jia, L.L. Lou, C. Zhang, Y. Zhang, S. Liu, Selective oxidation of benzyl alcohol to benzaldehyde with hydrogen peroxide over alkali-treated ZSM-5 zeolite catalysts, J. *Mol. Catal. A-Chem.*, **2009**, *306*, 123-129.
[52] J. Perez-Ramirez, D. Verboekend, A. Bonilla, and S. Abello, *Adv. Funct. Mater*, **2009**, 19, 3972-3979.
[53] K. Sadowska, K. Gora-Marek, M. Drozdek, P. Kustrowski, J. Datka, J. Martinez Triguero, F. Rey, *Microporous and Mesoporous Maters.*, **2013**,*168*, 195–205.
[54] A.N.C van Laak, L. Zhang, A.N. Parvulescu, P.C.A Bruijnincx, B.M. Weckhuysen, K.P. de Jong, P.E. *Catal. Today*, **2011**,*168*, 8-56.
[55] L. Wang, Z. Zhang, C. Yin, Z. Shan, F.S. Xiao, *Microporous Mesoporous Mater.*, **2010**, *131*, 58-67.

How to cite this manuscript: Sedigheh Rostami, Seyed Naser Azizi, Neda Asemi. "Preparing hierarchical nanoporous ZSM-5 zeolite via post-synthetic modification of zeolite synthesized from bagasse and its application for removal of Pb2+". *Eurasian Chemical Communications*, 2019, 20-42.